Electronic Supplementary Information (ESI) for: Photodynamics of alternative DNA base isoguanine

Gregory Gate,[a‡] Rafał Szabla,[*b,c‡] Michael Haggmark,[a] Jiří Šponer,[c] Andrzej L. Sobolewski[b] and Mattanjah S. de Vries[*a]

May 9, 2019

Assignment of key vibrational modes

Table 1 The key (anharmonic) vibrational frequencies in the spectral region tracked in the IR-UV hole burning experiments obtained at the B2PLYP/def2-TZVP level.

Vibration type	Theory (anharmonic) [cm^{-1}]
keto-N3,7	
symmetric NH_2 stretching (amino group)	3443
N3H stretching	3463
N7H stretching	3510
symmetric NH_2 stretching (amino group)	3554
keto-N1,9	
symmetric NH_2 stretching (amino group)	3438
N1H stretching	3467
N9H stretching	3493
asymmetric NH_2 stretching (amino group)	3581
keto-N3,9	
symmetric NH_2 stretching (amino group)	3425
N3H stretching	3455
N9H stretching	3491
asymmetric NH_2 stretching (amino group)	3535
keto-N1,7	
symmetric NH_2 stretching (amino group)	3431
N1H stretching	3442
N7H stretching	3495
asymmetric NH_2 stretching (amino group)	3533
enol-N7	
symmetric NH_2 stretching (amino group)	3439
N7H stretching	3510
asymmetric NH_2 stretching (amino group)	3542
OH stretching	3631
keto-N9	
symmetric NH_2 stretching (amino group)	3504
N9H stretching	3507
asymmetric NH_2 stretching (amino group)	3636
OH stretching	3637

Vertical excitation energy benchmarks

Table 2 Vertical excitation energies (in eV) of the four considered tautomers of isoG, computed using the ADC(2)/aug-cc-pVTZ method, assuming the ground-state minimum energy structures optimized at the B3LYP/def2-TZVPP level.

State / Transition		E_{exc}/[eV]	f_{osc}	λ/[nm]
		keto-N1,9		
S_1	$\pi\pi^*$	3.89	0.142	318.7
S_2	$\pi\sigma^*_{NH}$	4.71	$2.23 \cdot 10^{-3}$	263.2
S_3	$n_N\pi^*$	4.93	$2.27 \cdot 10^{-4}$	251.5
S_4	$\pi\sigma^*_{NH}$	5.20	$1.78 \cdot 10^{-4}$	238.4
S_5	$n_O\pi^*$	5.24	$3.94 \cdot 10^{-5}$	236.6
S_6	$\pi\pi^*$	5.35	0.176	231.7
		keto-N3,7		
S_1	$\pi\pi^*$	4.22	0.162	293.8
S_2	$n_O\pi^*$	4.77	$1.53 \cdot 10^{-3}$	259.9
S_3	$\pi\sigma^*_{NH}$	4.84	$1.16 \cdot 10^{-3}$	256.2
S_4	$n_N\pi^*$	5.11	$2.42 \cdot 10^{-3}$	242.6
S_5	$\pi\pi^*$	5.51	0.145	225.0
S_6	$\pi\sigma^*_{NH}$	5.66	$2.80 \cdot 10^{-3}$	219.1
		enol-N7		
S_1	$\pi\pi^*$	4.57	0.144	271.3
S_2	$n_N\pi^*$	4.84	$2.94 \cdot 10^{-3}$	256.2
S_3	$\pi\sigma^*_{NH}$	4.97	$5.46 \cdot 10^{-3}$	249.5
S_4	$\pi\pi^*$	5.62	$6.21 \cdot 10^{-2}$	220.6
S_5	$n\sigma^*_{NH}$	5.71	$1.52 \cdot 10^{-2}$	217.1
S_6	$\pi\sigma^*_{OH}$	5.81	$1.22 \cdot 10^{-3}$	213.4
		enol-N9		
S_1	$\pi\pi^*$	4.94	0.188	251.0
S_2	$n_N\pi^*$	5.35	$2.52 \cdot 10^{-3}$	231.7
S_3	$\pi\sigma^*_{NH}$	5.39	$3.45 \cdot 10^{-3}$	230.0
S_4	$\pi\pi^*$	5.45	0.113	227.5
S_5	$\pi\sigma^*_{NH}$	5.73	$7.36 \cdot 10^{-4}$	216.4
S_6	$n_N\pi^*$	6.07	$1.06 \cdot 10^{-3}$	204.3

Table 3 Vertical excitation energies (in eV) of the four considered tautomers of isoG, computed using the ADC(2)/aug-cc-pVTZ method, assuming the ground-state minimum energy structures optimized at the MP2/cc-pVTZ level.

State / Transition		E_{exc}/[eV]	f_{osc}	λ/[nm]
		keto-N1,9		
S_1	$\pi\pi^*$	3.84	0.138	322.9
S_2	$\pi\sigma^*_{NH}$	4.71	$2.15 \cdot 10^{-3}$	263.2
S_3	$n_N\pi^*$	4.89	$3.26 \cdot 10^{-4}$	253.5
S_4	$\pi\sigma^*_{NH}$	5.20	$2.65 \cdot 10^{-4}$	238.4
S_5	$n_O\pi^*$	5.22	$6.39 \cdot 10^{-5}$	237.5
S_6	$\pi\pi^*$	5.31	0.181	233.5
		keto-N3,7		
S_1	$\pi\pi^*$	4.22	0.169	293.8
S_2	$n_O\pi^*$	4.74	$2.05 \cdot 10^{-3}$	261.6
S_3	$\pi\sigma^*_{NH}$	4.88	$1.23 \cdot 10^{-3}$	254.1
S_4	$n_N\pi^*$	5.11	$2.66 \cdot 10^{-3}$	242.6
S_5	$\pi\pi^*$	5.55	0.104	223.4
S_6	$\pi\sigma^*_{NH}$	5.66	$3.16 \cdot 10^{-3}$	219.1
		enol-N7		
S_1	$\pi\pi^*$	4.56	0.145	275.5
S_2	$n_N\pi^*$	4.86	$2.83 \cdot 10^{-3}$	255.1
S_3	$\pi\sigma^*_{NH}$	5.03	$4.98 \cdot 10^{-3}$	246.5
S_4	$\pi\pi^*$	5.63	$6.38 \cdot 10^{-2}$	220.2
S_5	$n\sigma^*_{NH}$	5.79	$1.15 \cdot 10^{-2}$	214.1
S_6	$\pi\sigma^*_{OH}$	5.81	$5.04 \cdot 10^{-3}$	213.4
		enol-N9		
S_1	$\pi\pi^*$	4.90	0.188	253.0
S_2	$n_N\pi^*$	5.36	$2.69 \cdot 10^{-3}$	231.3
S_3	$\pi\sigma^*_{NH}$	5.41	$4.26 \cdot 10^{-3}$	229.2
S_4	$\pi\pi^*$	5.45	0.110	227.5
S_5	$\pi\sigma^*_{NH}$	5.76	$2.10 \cdot 10^{-3}$	215.3
S_6	$\pi\sigma^*$	6.11	$1.36 \cdot 10^{-2}$	202.9
S_7	$n_N\pi^*$	6.12	$7.79 \cdot 10^{-3}$	202.6

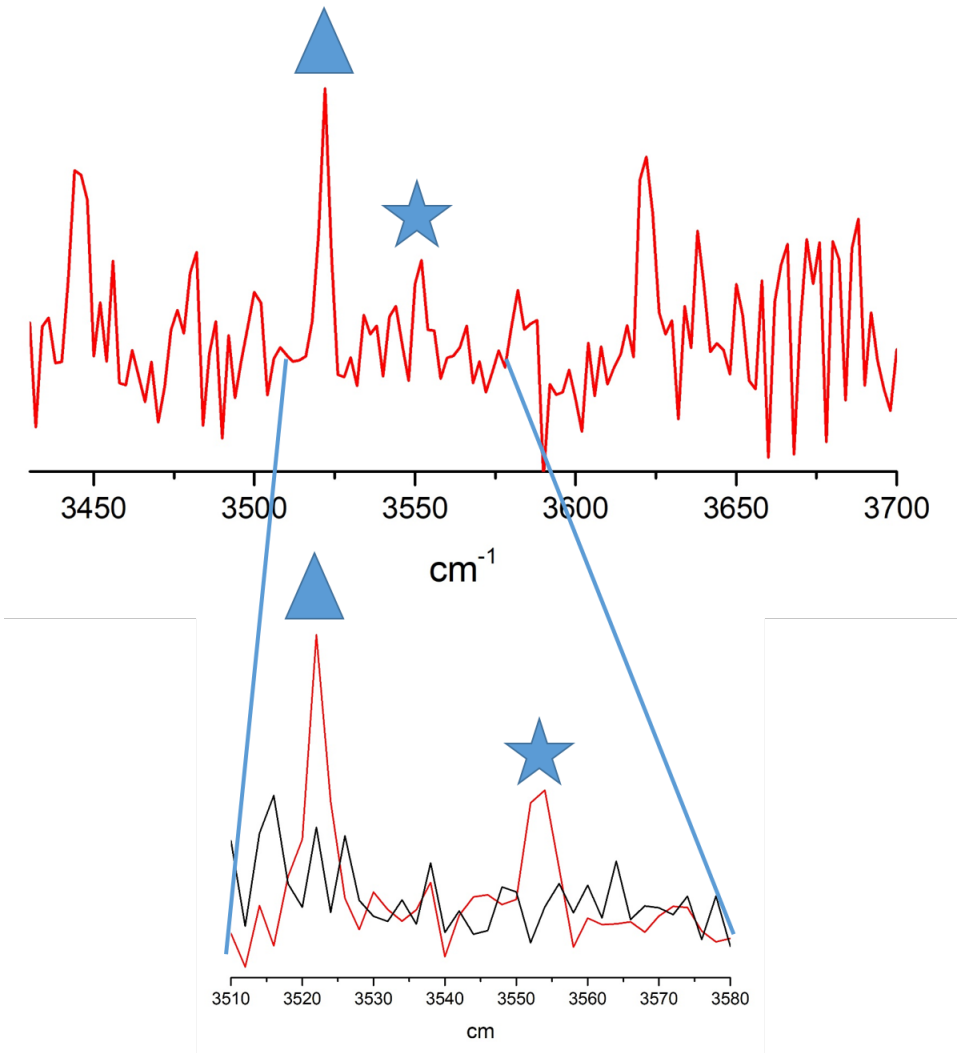

Fig. 1 Rescaled experimental data of the right spectrum of figure 2 (IR-UV double resonance spectrum probing at 34340 cm^{-1}). Red trace is burn signal and black is background signal. The peak marked by the triangle is at 3522 cm^{-1} and the peak marked by the star is at 3552 cm^{-1}. The inset displays the same experimental data, with the background signal displayed as well. This result demonstrates that the signal at 3552 cm^{-1} for the *enol*-N7 tautomer is a real peak.

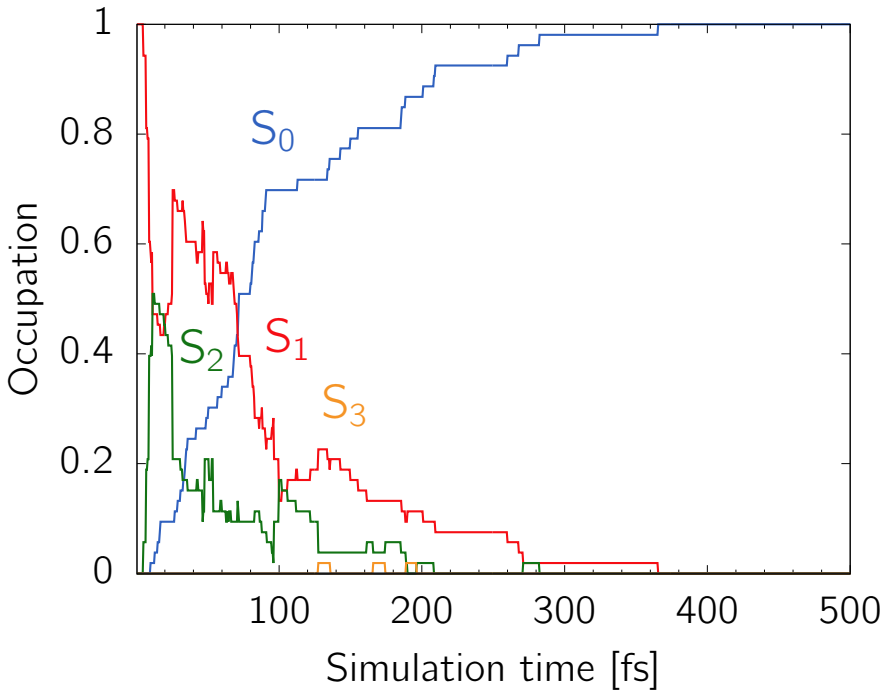

Fig. 2 Adiabatic populations of electronic states extracted from nonadiabatic molecular dynamics simulations performed for the *keto*-N1,9 tautomer. Very fast recovery of the electronic ground state is assigned here to the incorrect description of the topography of the $S_1(n\pi^*)/S_0$ state crossing in this particular tautomer (see the main article for more information).